MIMO-Assisted Space-Code-Division Multiple-Access: Linear Detectors and Performance Over Multipath Fading Channels

Lie-Liang Yang, *Senior Member, IEEE*

***Abstract*—In this contribution, we propose and investigate a multiple-input–multiple-output space-division, code-division multiple-access (MIMO SCDMA) scheme. The main objective is to improve the capacity of the existing direct-sequence (DS)-CDMA systems, for example, for supporting an increased number of users, by deploying multiple transmit and receive antennas in the corresponding systems and by using some advanced transmission and detection algorithms. In the proposed MIMO SCDMA system, each user can be distinguished jointly by its spreading code signature and its unique channel impulse response (CIR) transfer function referred to as spatial signature. Hence, the number of users might be supported by the MIMO SCDMA system and the corresponding achievable performance are determined by the degrees of freedom provided by both the code signatures and the spatial signatures, as well as by how efficiently the degrees of freedom are exploited. Specifically, the number of users supported by the proposed MIMO SCDMA can be significantly higher than the number of chips per bit, owing to the employment of space-division. In this contribution, space–time spreading is employed for configuring the transmitted signals. Three types of low-complexity linear detectors, namely, correlation, decorrelating, and minimum mean-square error (MMSE) are considered for detecting the MIMO SCDMA signals. The bit-error rate performance of the MIMO SCDMA system associated with these linear detectors are evaluated by simulations, when assuming that the MIMO SCDMA signals are transmitted over multipath Rayleigh-fading channels. Our study and simulation results show that MIMO SCDMA assisted by multiuser detection is capable of facilitating joint space–time despreading, multipath combining, and receiver diversity combining, while simultaneously suppressing the multiuser interfering signals.**

***Index Terms*—Code-division multiple access (CDMA), multipath-fading channels, multiple-input–multiple-output (MIMO), multiuser detection, space-division multiple access (SDMA), space–time spreading (STS).**

I. Introduction

In wireless communications, multiple-input–multiple-output (MIMO) systems equipped with multiple antennas at both the transmitter and receiver hold the promise of attaining substantial spectral efficiency improvements relative to what is achieved today [1]–[6]. Recently, MIMO systems have attracted intense research interests in the context of both MIMO theory and applications, as indicated, for example, by the special issues of [7]–[9] and the references therein. It is widely recognized that MIMO systems can be employed for achieving a high capacity [3], [5], [6] and a high diversity order [10], [11], for mitigating the effects of various types of interfering signals [12]–[14], and for supporting space-division multiple-access (SDMA) [14]–[17].

In wireless communications direct-sequence code-division multiple access (DS-CDMA) has been a typical multiple-access scheme in the second and third generations of wireless communications systems, and without any doubt, it will constitute an important candidate in the future generations of wireless communications systems. Hence, in this contribution, the application of MIMO principles in conjunction with DS-CDMA is investigated. Specifically, in the considered MIMO assisted DS-CDMA system, each of the mobile users employs multiple transmit antennas for achieving transmit diversity, with the aid of the space–time spreading (STS) schemes proposed in [18]. The common base-station (BS) receiver also employs multiple receive antennas, which might be functioned for multiple objectives, such as to achieve receiver diversity, to suppress various types of interfering signals, to support SDMA, etc. In the MIMO DS-CDMA system considered, each user is in correspondence with a unique DS spreading code, which is referred to as code signature, and also with a unique MIMO channel impulse response (CIR) transfer function referred to as spatial signature. Hence, a mobile user signal can be jointly distinguished by its code signature and spatial signature. Therefore, MIMO DS-CDMA can be termed as a multiple-access scheme using both code-division and space-division and, hence, we use the abbreviation of MIMO SCDMA for simplicity.

In [18], it has been demonstrated that the STS scheme is an open-loop transmit diversity scheme designed specifically for the CDMA systems employing DS spreading [18], [19]. The downlink performance of the CDMA systems using STS has been investigated in [18], when assuming orthogonal spreading codes and when the channel is modeled either as a flat or as a frequency-selective Rayleigh-fading channel in the absence of multiuser interference. By contrast, in [19], a broadband multicarrier DS-CDMA (MC DS-CDMA) scheme using STS has been proposed for downlink transmission and its performance has been investigated, when communicating over frequency-selective fading channels. Furthermore, in [20], a STS assisted downlink transmission scheme has been designed, which considers jointly the degrees of freedom provided by both the time-domain and the space-domain in a MIMO DS-CDMA systems. The performance of the proposed scheme has been investigated associated with various detection schemes, when the channel from any of the transmit antennas to any of the receive antennas

Manuscript received September 29, 2004; revised June 12, 2005.
The author is with the School of Electronics and Computer Science, University of Southampton, SO17 1BJ, U.K. (e-mail: lly@ecs.soton.ac.uk).
Digital Object Identifier 10.1109/JSAC.2005.858892

is modeled as independent flat fading channel. The analysis and results in [18]–[20] show that the STS scheme constitutes an attractive transmit diversity scheme, which is capable of attaining the maximal achievable transmit diversity gain without using extra spreading codes and without an increased transmit power.

In this contribution, the MIMO SCDMA system using STS is investigated, when considering the uplink transmission in a cellular-style system, since DS-CDMA has been mainly deployed in cellular systems. Specifically, the performance of a range of linear single-user and multiuser detectors (MUDs), namely, correlation, decorrelating, and minimum mean-square error (MMSE) detectors [21], for the synchronous MIMO SCDMA systems is investigated, when communicating over multipath Rayleigh-fading channels. Furthermore, it is well-recognized that, when multipath fading channel is considered, the DS-CDMA system using orthogonal spreading codes performs not as good as the system using some other types of nonorthogonal spreading codes, such as Gold sequences [1]. This is because, except the purely synchronous case, orthogonal spreading codes have an unsatisfactory correlation properties. Therefore, instead of using orthogonal spreading codes for the STS in the context of downlink case, in this contribution Gold sequences [22] are used for the STS in the considered MIMO SCDMA system.

The remainder of this contribution is organized as follows. Section II describes the MIMO SCDMA system using STS and the representation of the MIMO space–time DS-CDMA signal. Section III considers the linear detection of the MIMO SCDMA signals, where three linear detectors, namely, correlation, decorrelating, and MMSE that have been widely investigated in the literature, are extended for detecting the MIMO SCDMA signals. In Section IV, we provide a range of simulation results and, finally, in Section V, we present our conclusions.

II. System Description

A. Transmitted Signal

The MIMO system considered in this paper consists of U transmit antennas and V receive antennas. The transmitter schematic diagram of the kth user is shown in Fig. 1, where real-valued data symbols using binary phase-shift keying (BPSK) baseband modulation and real-valued spreading [18] were assumed. Note that the analysis in this contribution can be extended to the MIMO SCDMA systems using complex-valued data symbols, as well as complex-valued spreading. As shown in Fig. 1, at the transmitter side, the binary input data stream having a bit duration of T_b is serial-to-parallel (S-P) converted to U parallel substreams. The new bit duration of each parallel substream or the symbol duration becomes $T_s = UT_b$. After S-P conversion, the U parallel bits are direct-sequence spread using the STS schemes proposed in [18] with the aid of U pseudo-noise (PN) spreading sequences having a period of UN, where $N = T_b/T_c$ represents the number of chips per bit time-duration and T_c is the chip-duration of the PN spreading sequence. As seen in Fig. 1, following STS, the U parallel signals are mapped to the U transmit antennas, where the U parallel signals are carrier modulated and transmitted by the corresponding U antennas.

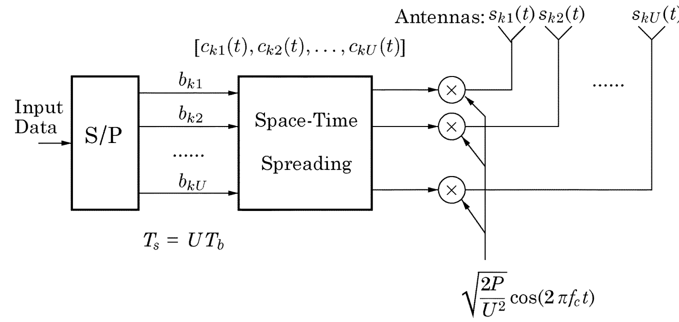

Fig. 1. Transmitter block diagram of the MIMO SCDMA system using space–time spreading.

As described above, we have assumed that the number of parallel data substreams, the number of PN spreading sequences used by the STS block of Fig. 1, and the number of transmit antennas are the same value, namely, U. These assumptions are supported by the research in [18], which shows that the STS scheme satisfying the above-mentioned conditions is capable of providing maximal transmit diversity without requiring extra STS spreading codes. Note that for the specific values of $U = 2$, 4, the above mentioned attractive STS schemes have been specified in [18]. In this contribution, we only investigate these attractive STS schemes.

For the sake of easy to follow, below the MIMO SCDMA system using two transmit antennas is first used as an example, in order to describe the principles of the MIMO SCDMA systems using STS. This special example is then extended to the general cases, where U transmit antennas are employed by the MIMO SCDMA system.

Based on the philosophy of STS as discussed in [18] and by referring to Fig. 1, for $U = 2$ transmit antenna case, the transmitted signal of the kth user within a data block of M symbol durations can be expressed as

$$\boldsymbol{s}_k(t) = \begin{bmatrix} s_{k1}(t) \\ s_{k2}(t) \end{bmatrix} = \sum_{m=0}^{M-1} \begin{bmatrix} \sqrt{\frac{2P}{2^2}}\,[b_{k1}(m)c_{k1}(t-mT_s) \\ \quad +b_{k2}(m)c_{k2}(t-mT_s)]\cos(2\pi f_c t + \phi_{k1}) \\ \sqrt{\frac{2P}{2^2}}\,[b_{k2}(m)c_{k1}(t-mT_s) \\ \quad -b_{k1}(m)c_{k2}(t-mT_s)]\cos(2\pi f_c t + \phi_{k2}) \end{bmatrix} \quad (1)$$

where P represents each user's transmitted power, which is constant for all users, $U \times U = 2 \times 2 = 2^2$ is a power normalization factor, where the first U is due to the U number of transmit antennas, while the second U is due to the symbol duration of $T_s = UT_b$. It can be shown that, after the normalization, we have $\int_0^{T_s} |s_k(t)|^2 dt = UE_b$, where $E_b = PT_b$ represents the energy per bit. In (1), $\boldsymbol{s}_k(t) = [s_{k1}(t)\ s_{k2}(t)]^T$—where T denotes vector or matrix transpose—represents the transmitted signal vector of the $U = 2$ transmit antennas, while M represents the number of symbols transmitted per block. Hence, each block transmits MU bits. As shown in (1), for the case of $U = 2$, the mth symbol contains two bits of $b_{k1}(m)$ and $b_{k2}(m)$, which are transmitted with the aid of the STS scheme based on two transmit antennas [18]. In this contribution, since frequency-selective multipath fading channels are considered, the STS sequences may be assumed the periodic PN sequences having a period of $T_s = UT_b = UNT_c$. The STS sequence waveform can be expressed in the form of $c_{ku}(t) = \sum_{j=0}^{UN-1} c_{ku}^j \psi_{T_c}(t - jT_c)$, $u = 1, 2, \ldots, U$, where c_{ku}^j assumes values of $+1$ or -1, while $\psi_{T_c}(t)$ is the chip waveform, which is defined over the interval $[0, T_c)$ and has the property of $\int_0^{T_c} \psi_{T_c}^2(t)dt = T_c$. Finally, in (1), f_c represents the carrier frequency and ϕ_{ku}, $u = 1, 2$ represents the initial phase with respect to the uth antenna of the kth user.

B. Channel Model

The $U = 2$ parallel subsignals in $\boldsymbol{s}_k(t) = [s_{k1}(t)\ s_{k2}(t)]^T$ seen in (1) are transmitted over frequency-selective fading channels, where signal transmitted from any transmit antenna to any receive antenna experiences independent frequency-selective Rayleigh fading. We assume that the channel is time-invariant over a data block time-duration, while experiences independent fading for different data blocks. Consequently, for a given data block, the complex low-pass equivalent representation of the CIR corresponding to the uth transmit antenna of user k and the vth receive antenna is given by [23]

$$h_{vu}^{(k)}(t)=\sum_{l=0}^{L-1} h_{vu}^{(k)}(l)\delta(t-lT_c),\ v=1,2,\ldots,V; u=1,2,\ldots,U \quad (2)$$

where $h_{vu}^{(k)}(l) = |h_{vu}^{(k)}(l)|\exp(j\phi_{vu}^{(k)}(l))$ and $\tau_{kl} = lT_c$ represent the attenuation factor and delay of the lth multipath component, respectively, while L is the total number of resolvable multipath components and $\delta(t)$ is the Kronecker Delta-function. We assume that the phases $\{\phi_{vu}^{(k)}(l)\}$ in (2) are independent identically distributed (i.i.d.) random variables uniformly distributed in the interval $[0, 2\pi)$, while the L multipath attenuations $\{|h_{vu}^{(k)}(l)|\}$ are independent Rayleigh random variables with a probability density function (pdf) of [23]

$$p_{\left|h_{vu}^{(k)}(l)\right|}(R) = \frac{2R}{\Omega}e^{-\frac{R^2}{\Omega}}, \quad R > 0 \quad (3)$$

where $\Omega = E[|h_{vu}^{(k)}(l)|^2]$ is the second moment of $h_{vu}^{(k)}(l)$.

We assume that the MIMO SCDMA system supports $K \geq 1$ number of users, which transmit signals synchronously on the block time-duration basis. Furthermore, we assume that the long-term average power received from each user's space–time signal is the same. Consequently, when the K users' signals obeying the form of (1) are transmitted over the MIMO channels conflicting frequency-selective fading characterized by (2), the received complex low-pass equivalent signal by the vth receive antenna can be expressed as

$$\begin{aligned} R_v(t) = &\sum_{k=1}^{K}\sum_{l=0}^{L-1}\sum_{m=0}^{M-1}\sqrt{\frac{P}{2}} \\ &\times \Big(h_{v1}^{(k)}(l)\left[b_{k1}(m)c_{k1}(t - mT_s - lT_c)\right. \\ &\quad \left.+b_{k2}(m)c_{k2}(t - mT_s - lT_c)\right] \\ &\quad + h_{v2}^{(k)}(l)\left[b_{k2}(m)c_{k1}(t - mT_s - lT_c)\right. \\ &\quad \left.-b_{k1}(m)c_{k2}(t-mT_s-lT_c)\right]\Big)+N_v(t) \end{aligned} \quad (4)$$

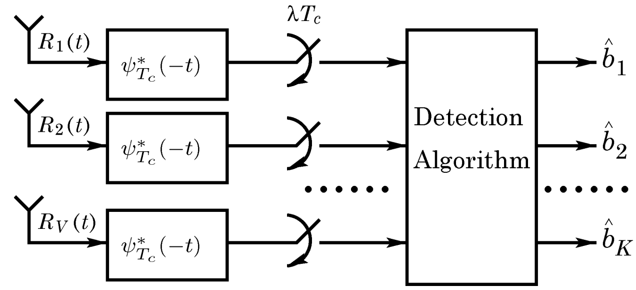

Fig. 2. Receiver schematic block diagram of the MIMO SCDMA systems.

where $v = 1, 2, \ldots, V$, $N_v(t)$ is the complex-valued additive white Gaussian noise (AWGN) received by the vth receive antenna, which has zero-mean and a single-sided spectrum density of N_0 per dimension. Note that, without loss of any generality, the initial phases seen in (1) have been absorbed into $h_{v1}^{(k)}(l)$ and $h_{v2}^{(k)}(l)$ in (4), respectively.

C. Representation of the Received Signals

The receiver structure for detection of the MIMO SCDMA signal is shown in Fig. 2. As shown in Fig. 2, the receiver comprises of V receive antennas. For each of the V receive antennas, the received signal is first passed through a filter matched to the transmitted chip-waveform of $\psi_{T_c}(t)$. Then, the output of the matched-filters are sampled at a rate of $1/T_c$. Hence, in a general MIMO SCDMA system using U transmit antennas, each receive antenna branch provides $(MUN + L - 1)$ samples corresponding to a data block, where $(L-1)$ is the result of channel delay, and the detector can collect a total of $V \times (MUN+L-1)$ samples from the V receive antennas. As shown in Fig. 2, the antenna output samples are sent to a detector, where the data transmitted by the K users is detected based on linear detection algorithms, which will be investigated in detail in our forthcoming discourse. Let us first derive the representation of the received MIMO space–time signal.

In the context of the vth receive antenna, as shown in Fig. 2, the λth sample obtained by sampling the chip-waveform matched-filter's output at the time-instant of $t = (\lambda + 1)T_c$ can be expressed as

$$y_v[\lambda] = \left(\sqrt{\frac{2P}{U^2}}T_c\right)^{-1} \int_{\lambda T_c}^{(\lambda+1)T_c} R_v(t)\psi_{T_c}^*(t)dt, \quad \lambda = 0, 1, \ldots, MUN + L - 2 \quad (5)$$

where * represents the complex conjugate.

Let

$$\begin{aligned} \boldsymbol{y}_v[m] &= [y_v[mUN], y_v[mUN + 1], \ldots, \\ &\qquad y_v\left[(m + 1)UN + L - 2\right]]^T \quad (6) \\ \boldsymbol{n}_v[m] &= [N_v[mUN], N_v[mUN + 1], \ldots, \\ &\qquad N_v\left[(m + 1)UN + L - 2\right]]^T \\ &\qquad m = 0, 1, 2, \ldots, M - 1 \quad (7) \end{aligned}$$

be the $(UN + L - 1)$-dimensional observation vector and noise vector corresponding to the vth receive antenna. Hence, the observation vector $\boldsymbol{y}_v[m]$ contains all the samples related to the STS symbols transmitted within the mth symbol duration by the K users. According to (5), it can be shown that the element $N_v[\lambda]$ in $\boldsymbol{n}_v[m]$ can be expressed as

$$N_v[\lambda] = \left(\sqrt{\frac{2P}{U^2}}T_c\right)^{-1} \int_{\lambda T_c}^{(\lambda+1)T_c} N_v(t)\psi^*_{T_c}(t)dt \qquad (8)$$

which is a complex Gaussian random variable with zero-mean and a variance of $U^2N_0/2E_c$ per dimension, where $E_c = PT_c$ represents the energy per chip. Upon substituting the received signal in the form of (4) into (5) and expressing in vector and matrix forms, it can be shown that $\boldsymbol{y}_v[m]$ can be expressed as

$$\boldsymbol{y}_v[0] = \sum_{k=1}^{K}\left\{\boldsymbol{C}_k[0]\boldsymbol{H}_{kv}\boldsymbol{b}_k[0] + \bar{\boldsymbol{C}}_k[1]\boldsymbol{H}_{kv}\boldsymbol{b}_k[1]\right\} + \boldsymbol{n}_v[0] \qquad (9)$$

$$\begin{aligned}\boldsymbol{y}_v[m] = \sum_{k=1}^{K}\{&\boldsymbol{C}_k[0]\boldsymbol{H}_{kv}\boldsymbol{b}_k[m] + \underline{\boldsymbol{C}}_k[-1]\boldsymbol{H}_{kv}\boldsymbol{b}_k[m-1]\\ &+\bar{\boldsymbol{C}}_k[1]\boldsymbol{H}_{kv}\boldsymbol{b}_k[m+1]\} + \boldsymbol{n}_v[m],\\ &m = 1, 2, \ldots, M-2\end{aligned} \qquad (10)$$

$$\begin{aligned}\boldsymbol{y}_v[M-1] = \sum_{k=1}^{K}\{&\boldsymbol{C}_k[0]\boldsymbol{H}_{kv}\boldsymbol{b}_k[M-1]\\ &+\underline{\boldsymbol{C}}_k[-1]\boldsymbol{H}_{kv}\boldsymbol{b}_k[M-2]\} + \boldsymbol{n}_v[M-1]\end{aligned} \qquad (11)$$

where $\boldsymbol{C}_k[0]$ is given by (12) shown at the bottom of the page, which is a $((UN+L-1) \times UL)$-dimensional matrix containing the U STS sequences of user k associated with the L multipath components. $\boldsymbol{C}_k[0]$ is corresponding to the current STS symbol received from user k. In (10) and (11), $\underline{\boldsymbol{C}}_k[-1]$ is given by (13) shown at the bottom of the page, which is a $((UN+L-1) \times UL)$-dimensional matrix constituted by the STS sequences of user k associated with the previous STS symbol of user k, but within its current symbol observation duration. In (13), $\mathbf{0}$ represents a zero matrix. Due to $\underline{\boldsymbol{C}}_k[-1]$, the current STS symbol of user k conflicts interference from the previous STS symbols of the K users in the system. In (9) and (10), $\bar{\boldsymbol{C}}_k[1]$ can be expressed as

$$\bar{\boldsymbol{C}}_k[1] = \begin{bmatrix} c_{k1}^0 & \ldots & c_{kU}^0 & 0 & \ldots & 0 & \ldots & 0 & \ldots & 0\\ c_{k1}^1 & \ldots & c_{kU}^1 & c_{k1}^0 & \ldots & c_{kU}^0 & \ldots & 0 & \ldots & 0\\ \vdots & \ddots & \vdots & \vdots & \ddots & \vdots & \ddots & \vdots & \ddots & \vdots\\ c_{k1}^{L-2} & \ldots & c_{kU}^{L-2} & c_{k1}^{L-3} & \ldots & c_{kU}^{L-3} & \ldots & 0 & \ldots & 0\\ & \mathbf{0} & & & \mathbf{0} & & \ldots & & \mathbf{0} & \end{bmatrix} \qquad (14)$$

which is also a $((UN+L-1)\times UL)$-dimensional matrix due to the following STS symbol of user k. Due to $\bar{\boldsymbol{C}}_k[1]$, the current STS symbol of user k conflicts interference from the following STS symbols of the whole K users.

In (9)–(11), the CIR matrix with respect to the kth user and the vth receive antenna can be expressed as

$$\boldsymbol{H}_{kv} = \left[\boldsymbol{H}_{kv}^T(0), \boldsymbol{H}_{kv}^T(1), \ldots, \boldsymbol{H}_{kv}^T(L-1)\right]^T \qquad (15)$$

where $\boldsymbol{H}_{kv}(l)$ for $l = 0, 1, \ldots, L-1$ are determined by the STS scheme employed. Specifically, for $U = 2$ and 4 and for real transmitted symbols, we have [18]

$$\boldsymbol{H}_{kv}(l) = \begin{bmatrix} h_{v1}^{(k)}(l) & h_{v2}^{(k)}(l)\\ -h_{v2}^{(k)}(l) & h_{v1}^{(k)}(l)\end{bmatrix}, \quad U = 2 \qquad (16)$$

$$\boldsymbol{C}_k[0] = \begin{bmatrix} c_{k1}^0 & \ldots & c_{kU}^0 & 0 & \ldots & 0 & \ldots & 0 & \ldots & 0\\ c_{k1}^1 & \ldots & c_{kU}^1 & c_{k1}^0 & \ldots & c_{kU}^0 & \ldots & 0 & \ldots & 0\\ \vdots & \ddots & \vdots & \vdots & \ddots & \vdots & \ddots & \vdots & \ddots & \vdots\\ \vdots & \ddots & \vdots & \vdots & \ddots & \vdots & \ddots & c_{k1}^0 & \ldots & c_{kU}^0\\ \vdots & \ddots & \vdots & \vdots & \ddots & \vdots & \ddots & \vdots & \ddots & \vdots\\ c_{k1}^{UN-1} & \ldots & c_{kU}^{UN-1} & c_{k1}^{UN-2} & \ldots & c_{kU}^{UN-2} & \ldots & c_{k1}^{UN-L} & \ldots & c_{kU}^{UN-L}\\ 0 & \ldots & 0 & c_{k1}^{UN-1} & \ldots & c_{kU}^{UN-1} & \ldots & c_{k1}^{UN-L+1} & \ldots & c_{kU}^{UN-L+1}\\ \vdots & \ddots & \vdots & \vdots & \ddots & \vdots & \ddots & \vdots & \ddots & \vdots\\ 0 & \ldots & 0 & 0 & \ldots & 0 & \ldots & c_{k1}^{UN-1} & \ldots & c_{kU}^{UN-1}\end{bmatrix} \qquad (12)$$

$$\underline{\boldsymbol{C}}_k[-1] = \begin{bmatrix} & \mathbf{0} & & & \mathbf{0} & & \ldots & & \mathbf{0} & \\ 0 & \ldots & 0 & c_{k1}^{UN-1} & \ldots & c_{kU}^{UN-1} & \ldots & c_{k1}^{UN-L+1} & \ldots & c_{kU}^{UN-L+1}\\ \vdots & \ddots & \vdots & \vdots & \ddots & \vdots & \ddots & \vdots & \ddots & \vdots\\ 0 & \ldots & 0 & 0 & \ldots & 0 & \ldots & c_{k1}^{UN-1} & \ldots & c_{kU}^{UN-1}\end{bmatrix} \qquad (13)$$

$$\boldsymbol{H}_{kv}(l) = \begin{bmatrix} h_{v1}^{(k)}(l) & h_{v2}^{(k)}(l) & h_{v3}^{(k)}(l) & h_{v4}^{(k)}(l) \\ -h_{v2}^{(k)}(l) & h_{v1}^{(k)}(l) & -h_{v4}^{(k)}(l) & h_{v3}^{(k)}(l) \\ -h_{v3}^{(k)}(l) & h_{v4}^{(k)}(l) & h_{v1}^{(k)}(l) & -h_{v2}^{(k)}(l) \\ -h_{v4}^{(k)}(l) & -h_{v3}^{(k)}(l) & h_{v2}^{(k)}(l) & h_{v1}^{(k)}(l) \end{bmatrix}, \quad U=4 \tag{17}$$

which are the STS schemes that will be used in our simulations in Section IV. Note that the representations of (9)–(11) can be readily extended to the cases, when using complex-valued data symbols, as well as complex-valued spreading.

Finally, in (9)–(11), $\boldsymbol{b}_k[m]$ is given by

$$\boldsymbol{b}_k[m] = [b_{k1}[m], b_{k2}[m], \ldots, b_{kU}[m]]^T, \quad k=1,2,\ldots,K;\ m=0,1,\ldots,M-1 \tag{18}$$

which is the mth STS symbol transmitted by the kth user.

Let

$$\boldsymbol{y}[m] = \left[\boldsymbol{y}_1[m]^T, \boldsymbol{y}_2[m]^T, \ldots, \boldsymbol{y}_V[m]^T\right]^T \tag{19}$$

represents the collection of all the samples of the V receive antennas. This collection contains the samples related to the symbols transmitted by the K users within the mth symbol duration. Then, $\boldsymbol{y}[m]$ can be expressed as

$$\boldsymbol{y}[m] = \sum_{k=1}^{K} \{(\boldsymbol{I}_V \otimes \boldsymbol{C}_k[0])\boldsymbol{H}_k\boldsymbol{b}_k[m] + (\boldsymbol{I}_V \otimes \underline{\boldsymbol{C}}_k[-1]) \times\boldsymbol{H}_k\boldsymbol{b}_k[m-1] + (\boldsymbol{I}_V \otimes \bar{\boldsymbol{C}}_k[1])\boldsymbol{H}_k\boldsymbol{b}_k[m+1]\} + \boldsymbol{n}[m] \tag{20}$$

where $\otimes$ represents the *Kronecker product* [24] operation

$$\boldsymbol{n}[m] = \left[\boldsymbol{n}_1[m]^T, \boldsymbol{n}_2[m]^T, \ldots, \boldsymbol{n}_V[m]^T\right]^T \tag{21}$$

represents a $(UN+L-1)V$-length noise vector, which has zero-mean and a covariance matrix

$$E\left[\boldsymbol{n}[m]\boldsymbol{n}[m]^H\right] = \frac{U^2N_0}{E_c}\boldsymbol{I}_{(UN+L-1)V} \tag{22}$$

and, furthermore, we have

$$\boldsymbol{H}_k = \left[\boldsymbol{H}_{k1}^T, \boldsymbol{H}_{k2}^T, \ldots, \boldsymbol{H}_{kV}^T\right]^T \tag{23}$$

which is a $ULV \times U$ matrix corresponding to the CIRs connecting the kth user to the V receive antennas.

Let

$$\boldsymbol{C}[0] = [(\boldsymbol{I}_V \otimes \boldsymbol{C}_1[0]), (\boldsymbol{I}_V \otimes \boldsymbol{C}_2[0]), \ldots, (\boldsymbol{I}_V \otimes \boldsymbol{C}_K[0])] \tag{24}$$

$$\underline{\boldsymbol{C}}[-1] = [(\boldsymbol{I}_V \otimes \underline{\boldsymbol{C}}_1[-1]), (\boldsymbol{I}_V \otimes \underline{\boldsymbol{C}}_2[-1]), \ldots, (\boldsymbol{I}_V \otimes \underline{\boldsymbol{C}}_K[-1])] \tag{25}$$

$$\bar{\boldsymbol{C}}[1] = \left[\left(\boldsymbol{I}_V \otimes \bar{\boldsymbol{C}}_1[1]\right), \left(\boldsymbol{I}_V \otimes \bar{\boldsymbol{C}}_2[1]\right), \ldots, \left(\boldsymbol{I}_V \otimes \bar{\boldsymbol{C}}_K[1]\right)\right] \tag{26}$$

$$\boldsymbol{H} = \text{diag}\{\boldsymbol{H}_1, \boldsymbol{H}_2, \ldots, \boldsymbol{H}_K\} \tag{27}$$

$$\boldsymbol{b}[m] = \left[\boldsymbol{b}_1^T[m], \boldsymbol{b}_2^T[m], \ldots, \boldsymbol{b}_K^T[m]\right]^T, \quad m=0,1,\ldots,M-1. \tag{28}$$

Then, (20) can also be written as

$$\boldsymbol{y}[m] = \boldsymbol{C}[0]\boldsymbol{H}\boldsymbol{b}[m] + \underline{\boldsymbol{C}}[-1]\boldsymbol{H}\boldsymbol{b}[m-1] + \bar{\boldsymbol{C}}[1]\boldsymbol{H}\boldsymbol{b}[m+1] + \boldsymbol{n}[m] \tag{29}$$

for $m=1,2,\ldots,M-2$. Note that, for $m=0$, the second component related to $\underline{\boldsymbol{C}}[-1]$ on the right-hand side of (29) should be removed. By contrast, for $m=M-1$ the third component containing $\bar{\boldsymbol{C}}[1]$ on the right-hand side of (29) should be removed. Let us now consider the linear detection of the STS assisted MIMO SCDMA signals.

III. Linear Detectors for MIMO SCDMA Systems Using Space–Time Spreading (STS)

In this section, we focus on the linear MUDs and their characteristics without imposing on any complexity restrictions, i.e., the detectors can be provided any information required. It is noteworthy that the received vector in (20) or (29) has some properties that are insightful for deriving efficient detection algorithms. These properties are summarized as follows.

1) The matrices $\boldsymbol{C}[0]$, $\underline{\boldsymbol{C}}[-1]$ and $\bar{\boldsymbol{C}}[1]$ in (24)–(26) are constituted by the DS spreading sequences of the K users, which represent the code signatures of the MIMO SCDMA system. By contrast, the $\boldsymbol{H}$ matrix in (27) is due to the CIRs of the MIMO system, which can be treated as the spatial signatures of the MIMO SCDMA system. Hence, each user in the MIMO SCDMA system considered can theoretically be distinguished by its corresponding code signature and/or spatial signature. Consequently, the number of users supported or the number of interferes suppressed by the MIMO SCDMA system is determined by the degrees of freedom, which is defined by the product of the number of chips per bit N, the number of transmit antennas U, and the number of receive antennas V, i.e., by NUV.
2) $\boldsymbol{C}[0]$, $\underline{\boldsymbol{C}}[-1]$ and $\bar{\boldsymbol{C}}[1]$ in (24)–(26) are time invariant matrices, while $\boldsymbol{H}$ in (27) is a time-variant matrix.
3) Since we assumed that the fading from each transmit antenna to any of the receive antennas was independent, the rank of $\boldsymbol{H}$ is, hence, column full with a probability one, i.e., we have $\text{rank}(\boldsymbol{H}) = UK$. Furthermore, it can be shown that we can design a $\boldsymbol{C}[0]$, so that it obeys

$$\text{rank}(\boldsymbol{C}[0]\boldsymbol{H}) = \min\{(UN+L-1)V, UK\}. \tag{30}$$

Hence, based on $\boldsymbol{C}[0]\boldsymbol{H}$, the detector is capable of distinguishing up to K number of users, provided that $KU \leq (UN+L-1)V$ or $K \leq (UN+L-1)V/U$.
4) The ranks of $\underline{\boldsymbol{C}}[-1]$ and $\bar{\boldsymbol{C}}[1]$ obey

$$\text{rank}(\underline{\boldsymbol{C}}[-1]) = \text{rank}\left(\bar{\boldsymbol{C}}[1]\right) \leq \min\{V(L-1), UK(L-1)\} \tag{31}$$

and the ranks of $\underline{\boldsymbol{C}}[-1]\boldsymbol{H}$ and $\bar{\boldsymbol{C}}[1]\boldsymbol{H}$ satisfy

$$\text{rank}(\underline{\boldsymbol{C}}[-1]\boldsymbol{H}) = \text{rank}\left(\bar{\boldsymbol{C}}[1]\boldsymbol{H}\right) \leq \min\{V(L-1), UK(L-1), UK\}. \tag{32}$$

The intersymbol interference (ISI) due to the delay-spread of the fading channels can be suppressed, provided that there are sufficient degrees of freedom in the received vector $\boldsymbol{y}[m]$ seen in (20) or (29).

5) The $\boldsymbol{H}$ matrix has the property of

$$\boldsymbol{H}^H\boldsymbol{H} = \text{diag}\left\{\boldsymbol{H}_1^H\boldsymbol{H}_1, \boldsymbol{H}_2^H\boldsymbol{H}_2, \ldots, \boldsymbol{H}_K^H\boldsymbol{H}_K\right\} \quad (33)$$

where

$$\begin{aligned}\boldsymbol{H}_k^H\boldsymbol{H}_k &= \sum_{v=1}^{V}\boldsymbol{H}_{kv}^H\boldsymbol{H}_{kv}\\ &= \sum_{v=1}^{V}\sum_{l=0}^{L-1}\boldsymbol{H}_{kv}^H(l)\boldsymbol{H}_{kv}(l),\ k = 1, 2, \ldots, K \quad (34)\end{aligned}$$

Furthermore, for the $\boldsymbol{H}_{kv}(l)$ given by (16) and (17), we have, respectively

$$\mathcal{R}\left(\boldsymbol{H}_k^H\boldsymbol{H}_k\right) = \sum_{v=1}^{V}\sum_{l=0}^{L-1}\left(\left|h_{v1}^{(k)}(l)\right|^2 + \left|h_{v2}^{(k)}(l)\right|^2\right)\boldsymbol{I}_2 \quad (35)$$

$$\begin{aligned}\mathcal{R}\left(\boldsymbol{H}_k^H\boldsymbol{H}_k\right) = \sum_{v=1}^{V}\sum_{l=0}^{L-1}\Bigg(\left|h_{v1}^{(k)}(l)\right|^2 + \left|h_{v2}^{(k)}(l)\right|^2\\ + \left|h_{v3}^{(k)}(l)\right|^2 + \left|h_{v4}^{(k)}(l)\right|^2\Bigg)\boldsymbol{I}_4,\ k=1,2,\ldots,K\end{aligned} \quad (36)$$

where $\mathcal{R}(x)$ represents the real part of x.

Based on the above-listed properties associated with MIMO SCDMA, let us now discuss the linear detection of the MIMO SCDMA signals. Let the output of a linear detector be expressed by

$$\boldsymbol{z}[m] = \left[\boldsymbol{z}_1^T[m], \boldsymbol{z}_2^T[m], \ldots, \boldsymbol{z}_K^T[m]\right]^T \quad (37)$$

$$\boldsymbol{z}_k[m] = [z_{k1}[m], z_{k2}[m], \ldots, z_{kU}[m]]^T, k = 1, \ldots, K \quad (38)$$

which consists of the decision variables for the data-bits transmitted by the K users during the mth symbol duration, $\boldsymbol{z}_k[m]$ contains the decision variables for $\boldsymbol{b}_k[m]$ in (18) and $\hat{b}_{ki}[m] = \text{sgn}(\mathcal{R}(z_{ki}[m]))$. For a linear detector, the received space–time vector $\boldsymbol{y}[m]$ given in (20) or (29) is linearly processed to form the decision variables $\boldsymbol{z}[m]$, which can be expressed as

$$\boldsymbol{z}[m] = \boldsymbol{W}^H\boldsymbol{y}[m] \quad (39)$$

where the processing matrix $\boldsymbol{W}$ can be derived based on the specific constraints imposed on the detector, as shown below. Note that, in our forthcoming discourse, we often refer to the first user as the reference user and our objective is to detect the information transmitted by this reference user.

A. Correlation Detector

The correlation detector is derived, when assuming that the receiver is only capable of obtaining the knowledge of the desired user, including the STS sequences (code signature) and the CIRs (spatial signature) of the desired user. Specifically, for the correlation detector, the decision variable $\boldsymbol{z}[m]$ is obtained by despreading the received space–time signal $\boldsymbol{y}[m]$ using $\boldsymbol{W} = \boldsymbol{C}[0]\boldsymbol{H}$, i.e., we have

$$\boldsymbol{z}[m] = (\boldsymbol{C}[0]\boldsymbol{H})^H\boldsymbol{y}[m] = \boldsymbol{H}^H\boldsymbol{C}^T[0]\boldsymbol{y}[m] \quad (40)$$

which first carries out the despreading in the time-domain using the code signature of $\boldsymbol{C}[0]$, followed by the despreading in the space-domain using the spatial signature $\boldsymbol{H}$.

The correlation detector is a single-user detector, which treats both multiuser signals and ISI signals simply as background noise. The correlation detector usually conflicts severe interference generated by the other users in the system, as well as by the transmission delay of wireless channels. This becomes explicit when we express the decision variable $z_{11}[m]$, which is corresponding to $b_{11}[m]$, in detail as

$$z_{11}[m] = \left(\boldsymbol{H}_1^H\left(\boldsymbol{I}_v \otimes \boldsymbol{C}_1[0]\right)^T\boldsymbol{y}[m]\right)_1 \quad (41)$$

where $(\boldsymbol{x})_1$ represents the first element of the vector $\boldsymbol{x}$. Upon substituting (20) into (41), we obtain

$$\begin{aligned}z_{11}[m] =& \left(\boldsymbol{H}_1^H\left(\boldsymbol{I}_v \otimes \boldsymbol{C}_1[0]\right)^T\left(\boldsymbol{I}_V \otimes \boldsymbol{C}_1[0]\right)\boldsymbol{H}_1\boldsymbol{b}_1[m]\right)_1\\ &+ \Bigg(\sum_{k=2}^{K}\boldsymbol{H}_1^H\left(\boldsymbol{I}_v \otimes \boldsymbol{C}_1[0]\right)^T\left(\boldsymbol{I}_V \otimes \boldsymbol{C}_k[0]\right)\boldsymbol{H}_k\boldsymbol{b}_k[m]\\ &\quad + \sum_{k=1}^{K}\boldsymbol{H}_1^H\left(\boldsymbol{I}_v \otimes \boldsymbol{C}_1[0]\right)^T\left(\boldsymbol{I}_V \otimes \underline{\boldsymbol{C}}_k[-1]\right)\\ &\quad \times \boldsymbol{H}_k\boldsymbol{b}_k[m-1]\\ &\quad + \sum_{k=1}^{K}\boldsymbol{H}_1^H\left(\boldsymbol{I}_v \otimes \boldsymbol{C}_1[0]\right)^T\left(\boldsymbol{I}_V \otimes \bar{\boldsymbol{C}}_k[1]\right)\\ &\quad \times\boldsymbol{H}_k\boldsymbol{b}_k[m+1] + \boldsymbol{H}_1^H\left(\boldsymbol{I}_v \otimes \boldsymbol{C}_1[0]\right)^T\boldsymbol{n}[m]\Bigg)_1\\ =& \left(\boldsymbol{H}_1^H\left(\boldsymbol{I}_v \otimes \boldsymbol{C}_1[0]\right)^T\left(\boldsymbol{I}_V \otimes \boldsymbol{C}_1[0]\right)\boldsymbol{H}_1\boldsymbol{b}_1[m]\right)_1\\ &+ \text{MUI} + \text{ISI}. \end{aligned} \quad (42)$$

According to the properties of the *Kronecker Product*,[1] (42) can be written as

$$z_{11}[m] = \left(\boldsymbol{H}_1^H\left(\boldsymbol{I}_V \otimes \boldsymbol{C}_1^T[0]\boldsymbol{C}_1[0]\right)\boldsymbol{H}_1\boldsymbol{b}_1[m]\right)_1 + \text{MUI} + \text{ISI} \quad (43)$$

which implies that the space–time signals received by the V receive antennas can be despread separately. Let $\overline{\text{diag}}(\boldsymbol{C}_1^T[0]\boldsymbol{C}_1[0])$ be the matrix obtained by setting the diagonal elements in $\boldsymbol{C}_1^T[0]\boldsymbol{C}_1[0]$ to be zeros. Then, (43) can be expressed as

$$\begin{aligned}z_{11}[m] =& \left(\boldsymbol{H}_1^H\left(\boldsymbol{I}_V \otimes \left[UN\boldsymbol{I}_{UL} + \overline{\text{diag}}\left(\boldsymbol{C}_1^T[0]\boldsymbol{C}_1[0]\right)\right]\right)\boldsymbol{H}_1\boldsymbol{b}_1[m]\right)_1\\ &+ \text{MUI} + \text{ISI}\\ =& UN\left(\boldsymbol{H}_1^H(\boldsymbol{I}_V \otimes \boldsymbol{I}_{UL})\boldsymbol{H}_1\boldsymbol{b}_1[m]\right)_1\\ &+ \underbrace{\left(\boldsymbol{H}_1^H\left(\boldsymbol{I}_V \otimes \overline{\text{diag}}\left(\boldsymbol{C}_1^T[0]\boldsymbol{C}_1[0]\right)\right)\boldsymbol{H}_1\boldsymbol{b}_1[m]\right)_1}_{\text{SI:Self}-\text{interference}}\\ &+ \text{MUI} + \text{ISI}\\ =& \left(UN\boldsymbol{H}_1^H\boldsymbol{H}_1\boldsymbol{b}_1[m]\right)_1 + \text{SI} + \text{MUI} + \text{ISI}\\ =& \left(UN\sum_{v=1}^{V}\sum_{l=0}^{L-1}\boldsymbol{H}_{kv}^H(l)\boldsymbol{H}_{kv}(l)\boldsymbol{b}_1[m]\right)_1\\ &+ \text{SI} + \text{MUI} + \text{ISI}.\end{aligned} \quad (44)$$

[1] $(\boldsymbol{A} \otimes \boldsymbol{B})^T = (\boldsymbol{A}^T \otimes \boldsymbol{B}^T)$ and $(\boldsymbol{A} \otimes \boldsymbol{B})(\boldsymbol{C} \otimes \boldsymbol{D}) = (\boldsymbol{AC} \otimes \boldsymbol{BD})$ [24], [25].

Furthermore, it can be shown that, when the STS scheme using $U = 2$ transmit antennas is employed, the decision variable for $b_{11}[m]$ is given by

$$z_{11}[m] = 2N \sum_{v=1}^{V} \sum_{l=0}^{L-1} \left[\left| h_{v1}^{(k)}(l) \right|^2 + \left| h_{v2}^{(k)}(l) \right|^2 \right] b_{11}[m] + \text{SI} + \text{MUI} + \text{ISI} \quad (45)$$

which implies that the correlation detector is in fact a space–time RAKE-like receiver using the maximal-ratio combining (MRC). The diversity order achieved is $2VL$, where the factor of two is contributed by two transmit antennas indicated in (45) by the sum of $(|h_{v1}^{(k)}(l)|^2 + |h_{v2}^{(k)}(l)|^2)$. Additionally, in (45), the factor $2N$ is due to the STS using two transmit antennas.

B. Decorrelating Multiuser Detector (MUD)

The decorrelating MUD is capable of suppressing the multiuser interference (MUI), as well as the ISI [21]. For the proposed MIMO SCDMA system, the decorrelating MUD may be implemented as follows. First, when the ISI associated with $\boldsymbol{b}[m-1]$ and $\boldsymbol{b}[m+1]$ in (29) is ignored in the detection, in order that the effective degrees of freedom can be saved, for example, for the sake of supporting more users. The decorrelating detector can be implemented by first despreading the received vector $\boldsymbol{y}[m]$ using both the code signature $\boldsymbol{C}[0]$ and the spatial signature $\boldsymbol{H}$. The resulted signal is expressed by (40). Then, the decision variable is obtained by multiplying the despread signal using the inverse of space–time correlation matrix $\boldsymbol{R}_0 = (\boldsymbol{C}[0]\boldsymbol{H})^H (\boldsymbol{C}[0]\boldsymbol{H})$. Hence, we have

$$\begin{aligned} \boldsymbol{z}[m] &= \boldsymbol{R}_0^{-1} \left(\boldsymbol{C}[0]\boldsymbol{H}\right)^H \boldsymbol{y}[m] \\ &= \left(\boldsymbol{H}^H \boldsymbol{C}^T[0]\boldsymbol{C}[0]\boldsymbol{H}\right)^{-1} \boldsymbol{H}^H \boldsymbol{C}^T[0]\boldsymbol{y}[m] \end{aligned} \quad (46)$$

and, correspondingly, the weight matrix $\boldsymbol{W}$ in (39) is given by

$$\boldsymbol{W} = \boldsymbol{C}[0]\boldsymbol{H} \left(\boldsymbol{H}^H \boldsymbol{C}^T[0]\boldsymbol{C}[0]\boldsymbol{H}\right)^{-1}. \quad (47)$$

Second, when the MIMO SCDMA system has sufficient degrees of freedom, the decorrelating MUD can also be implemented by suppressing both the MUI and ISI simultaneously. We may also need to suppress the MUI and ISI jointly, when the delay-spread of wireless channels is high, which results in high ISI. When the decorrelating detector attempts to suppress both the MUI and ISI, the received space–time signal vector $\boldsymbol{y}[m]$ in (29) can be expressed as

$$\boldsymbol{y}[m] = \mathcal{C}\mathcal{H}\boldsymbol{b} + \boldsymbol{n}[m] \quad (48)$$

where

$$\mathcal{C} = \left[\boldsymbol{C}^T[0], \underline{\boldsymbol{C}}[-1], \overline{\boldsymbol{C}}[1]\right] \quad (49)$$

$$\mathcal{H} = \boldsymbol{I}_3 \otimes \boldsymbol{H} \quad (50)$$

$$\boldsymbol{b} = [\boldsymbol{b}[m], \boldsymbol{b}[m-1], \boldsymbol{b}[m+1]]^T. \quad (51)$$

As shown in (13) and (14), the matrices $\underline{\boldsymbol{C}}[-1]$ and $\overline{\boldsymbol{C}}[1]$ contain many correlated columns. Hence, the rank of $\mathcal{C}\mathcal{H}$ in (48) obeys $UK \leq \Sigma = \text{rank}(\mathcal{C}\mathcal{H}) < 3\,UK$. In this case, the weight matrix $\boldsymbol{W}$ corresponding to the decorrelating MUD is given by [21, pp. 241–242]

$$\boldsymbol{W} = \mathcal{C}\mathcal{H}(\mathcal{H}^H \mathcal{C}^T \mathcal{C}\mathcal{H})^\dagger \quad (52)$$

where † represents the pseudo-inverse or the *Moore–Penrose* generalized inverse [25]. Let the singular value decomposition (SVD) of $\mathcal{C}\mathcal{H}$ be expressed as

$$\mathcal{C}\mathcal{H} = \mathcal{U}\Lambda_\Sigma \mathcal{V}^H \quad (53)$$

where $\mathcal{U}$ and $\mathcal{V}$ are $(UN+L-1)V$-by-$(UN+L-1)V$ and $3UK$-by-$3UK$ unitary matrices, respectively, so that we have

$$\mathcal{U}^H \mathcal{C}\mathcal{H}\mathcal{V} = \Lambda_\Sigma = \begin{bmatrix} \boldsymbol{\Sigma} & \boldsymbol{0} \\ \boldsymbol{0} & \boldsymbol{0} \end{bmatrix} \quad (54)$$

and $\boldsymbol{\Sigma}$ is a diagonal matrix containing the singular values of $\mathcal{C}\mathcal{H}$

$$\boldsymbol{\Sigma} = \text{diag}\{\sqrt{\lambda_1}, \sqrt{\lambda_2}, \ldots, \sqrt{\lambda_\Sigma}\} \quad (55)$$

where $\{\lambda_i\}$ are the eigenvalues of the Hermitian matrix $\mathcal{H}^H \mathcal{C}^T \mathcal{C}\mathcal{H}$.

Upon substituting (53) into (52), we obtain

$$\begin{aligned} \boldsymbol{W} &= \mathcal{U}\Lambda_\Sigma \mathcal{V}^H (\mathcal{V}\Lambda_\Sigma \mathcal{U}^H \mathcal{U}\Lambda_\Sigma \mathcal{V}^H)^\dagger \\ &= \mathcal{U}\Lambda_\Sigma \mathcal{V}^H \left(\mathcal{V}\Lambda_\Sigma^2 \mathcal{V}^H\right)^\dagger = \mathcal{U}\Lambda_\Sigma^{-1}\mathcal{V}^H \end{aligned} \quad (56)$$

where

$$\Lambda_\Sigma^{-1} = \begin{bmatrix} \boldsymbol{\Sigma}^{-1} & \boldsymbol{0} \\ \boldsymbol{0} & \boldsymbol{0} \end{bmatrix}. \quad (57)$$

Finally, the decision variable vector is given by

$$\boldsymbol{z} = \boldsymbol{W}^H \boldsymbol{y}[m] = \mathcal{V}\Lambda_\Sigma^{-1}\mathcal{U}^H \boldsymbol{y}[m] \quad (58)$$

where the first UK elements are chosen for detecting the STS symbols, $\boldsymbol{b}[m]$, transmitted by the K users within the mth STS symbol duration.

C. MMSE Detector

In the context of the MMSE detector, we assume that the first user is the desired user or reference user. The objective of the MMSE detector is to detect symbol $\boldsymbol{b}_1[m]$ transmitted by the desired user within the mth symbol duration. When the MMSE detector is considered, the weight matrix $\boldsymbol{W}$ is chosen such that the mean-square error (MSE) between the transmitted symbol vector $\boldsymbol{b}_1[m]$ and its estimate $\hat{\boldsymbol{b}}_1[m]$ is minimized. It is well known that the optimum solution in MMSE sense can be expressed as [26]

$$\boldsymbol{W}_o = \boldsymbol{R}_y^{-1}\boldsymbol{R}_{yb_1} \quad (59)$$

where $\boldsymbol{R}_y$ is the autocorrelation matrix of the received space–time vector $\boldsymbol{y}[m]$, while $\boldsymbol{R}_{yb_1}$ is the cross-correlation matrix between the received space–time vector $\boldsymbol{y}[m]$ and the desired symbol vector $\boldsymbol{b}_1[m]$. They can be expressed, respectively, as

$$\boldsymbol{R}_y = E\left[\boldsymbol{y}[m]\boldsymbol{y}^H[m]\right], \quad \boldsymbol{R}_{yb_1} = E\left[\boldsymbol{y}[m]\boldsymbol{b}_1^T[m]\right]. \quad (60)$$

When the channel information in terms of the spatial-signature $\boldsymbol{H}$ and the code signature $\boldsymbol{C}$ are available at the receiver, the autocorrelation matrix $\boldsymbol{R}_y$ can be obtained by substituting (20) into (60) and by considering that all information symbols are transmitted independently, which yields

$$\begin{aligned}\boldsymbol{R}_y = &\sum_{k=1}^{K}\Big\{(\boldsymbol{I}_V\otimes\boldsymbol{C}_k[0])\,\boldsymbol{H}_k\boldsymbol{H}_k^H\left(\boldsymbol{I}_V\otimes\boldsymbol{C}_k^T[0]\right)\\ &+(\boldsymbol{I}_V\otimes\underline{\boldsymbol{C}}_k[-1])\,\boldsymbol{H}_k\boldsymbol{H}_k^H\left(\boldsymbol{I}_V\otimes\underline{\boldsymbol{C}}_k^T[-1]\right)\\ &+\left(\boldsymbol{I}_V\otimes\bar{\boldsymbol{C}}_k[1]\right)\boldsymbol{H}_k\boldsymbol{H}_k^H\left(\boldsymbol{I}_V\otimes\bar{\boldsymbol{C}}_k^T[1]\right)\Big\}\\ &+\frac{U^2N_0}{E_c}\boldsymbol{I}_{(UN+L-1)V}\\ =&\,(\boldsymbol{I}_V\otimes\boldsymbol{C}_1[0])\,\boldsymbol{H}_1\boldsymbol{H}_1^H\left(\boldsymbol{I}_V\otimes\boldsymbol{C}_1^T[0]\right)+\boldsymbol{\Sigma}_I \qquad (61)\end{aligned}$$

where $\boldsymbol{\Sigma}_I$ includes the autocorrelation of the MUI, ISI, as well as the background noise. The cross-correlation matrix between the received space–time vector $\boldsymbol{y}[m]$ and the desired symbol vector $\boldsymbol{b}_1[m]$ can be expressed as

$$\boldsymbol{R}_{yb_1} = (\boldsymbol{I}_V\otimes\boldsymbol{C}_1[0])\,\boldsymbol{H}_1. \qquad (62)$$

Consequently, the optimum weight matrix can be expressed as

$$\begin{aligned}\boldsymbol{W}_o =& \boldsymbol{R}_y^{-1}\boldsymbol{R}_{yb_1}\\ =&\left[(\boldsymbol{I}_V\otimes\boldsymbol{C}_1[0])\,\boldsymbol{H}_1\boldsymbol{H}_1^H\left(\boldsymbol{I}_V\otimes\boldsymbol{C}_1^T[0]\right)+\boldsymbol{\Sigma}_I\right]^{-1}\\ &\times(\boldsymbol{I}_V\otimes\boldsymbol{C}_1[0])\,\boldsymbol{H}_1. \qquad (63)\end{aligned}$$

When invoking the *matrix inverse lemma* [24, pp. 1348], it can be shown that we have

$$\begin{aligned}\boldsymbol{W}_o =& \boldsymbol{\Sigma}_I^{-1}(\boldsymbol{I}_V\otimes\boldsymbol{C}_1[0])\,\boldsymbol{H}_1\Big[\boldsymbol{H}_1^H\left(\boldsymbol{I}_V\otimes\boldsymbol{C}_1^T[0]\right)\\ &\times\boldsymbol{\Sigma}_I^{-1}(\boldsymbol{I}_V\otimes\boldsymbol{C}_1[0])\,\boldsymbol{H}_1+\boldsymbol{I}_U\Big]^{-1}. \qquad (64)\end{aligned}$$

Define the normalized MMSE as

$$\mathrm{MMSE} = 1-\frac{1}{U}\mathrm{Trace}\left(\boldsymbol{R}_{yb_1}^H\boldsymbol{W}_o\right). \qquad (65)$$

Then, it can be shown that we have

$$\begin{aligned}\mathrm{MMSE} =& \frac{1}{U}\mathrm{Trace}\Big(\Big[\boldsymbol{H}_1^H\left(\boldsymbol{I}_V\otimes\boldsymbol{C}_1^T[0]\right)\\ &\times\boldsymbol{\Sigma}_I^{-1}(\boldsymbol{I}_V\otimes\boldsymbol{C}_1[0])\,\boldsymbol{H}_1+\boldsymbol{I}_U\Big]^{-1}\Big). \qquad (66)\end{aligned}$$

In comparison with the correlation detector in Section III-A and the decorrelating detector in Section III-B, the MMSE MUD is capable of suppressing both the MUI and ISI, provided that the MIMO SCDMA system has sufficient degrees of freedom. The MMSE MUD can also efficiently suppress the background noise. Furthermore, the MMSE scheme can readily be implemented using adaptive techniques [24], [26]. Let us now show some performance results for the proposed MIMO SCDMA system.

IV. Performance Examples

In this section. we provide a range of simulation results, in order to illustrate and compare the achievable performance of the MIMO SCDMA system in conjunction with various detection schemes, as considered in Sections III. In our simulation examples, we assumed that the Gold sequences having a period of $N = 31$ were employed for implementing the STS. Since the total number of Gold sequences having the period of $N = 31$ is $N + 2 = 33$ [22], and also since the MIMO SCDMA system may support up to NV users, the same Gold sequence may be assigned to more than one users, when the number of users supported exceeds $N + 2$. Additionally, as shown in Section II, the length of the STS sequences required is UN and each user requires U STS codes. In our simulation examples, these UN-length STS sequences of a given user were obtained by concatenating the assigned N-length Gold sequence with the U-length Walsh Hadamard codes. Specifically, let $\boldsymbol{c}_k$ be the Gold sequence assigned to the kth user. Then, for $U = 2$ and 4, the STS sequences of the kth user are given by

$$\begin{bmatrix}+1 & +1\\ +1 & -1\end{bmatrix}\otimes\boldsymbol{c}_k,\qquad \begin{bmatrix}+1 & +1 & +1 & +1\\ +1 & +1 & -1 & -1\\ +1 & -1 & +1 & -1\\ +1 & -1 & -1 & +1\end{bmatrix}\otimes\boldsymbol{c}_k. \qquad (67)$$

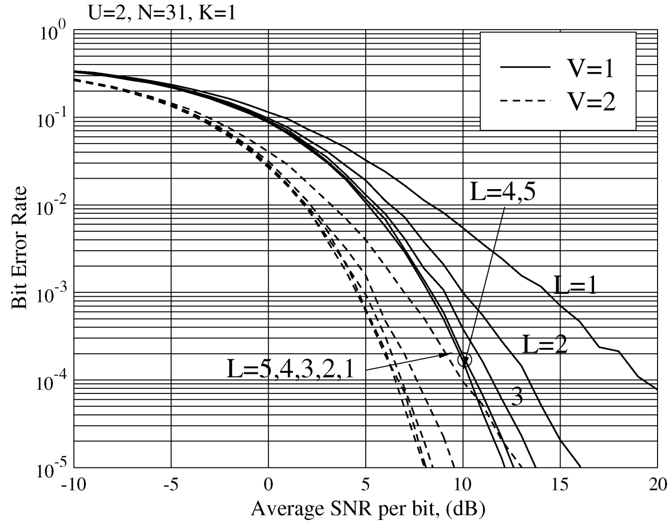

Fig. 3. BER performance of the single-user MIMO SCDMA system using $U = 2$ transmit antennas, $V = 1$ or two receive antennas, and $N = 31$ chips per bit duration, when communicating over Rayleigh-fading channels having $L = 1,2,3,4,5$ multipath components.

In Figs. 3 and 4. the bit-error rate (BER) performance of the single-user MIMO SCDMA systems was evaluated, when assuming various number of transmit antennas of U, various number of multipath components of L and various number of receive antennas of V. In principles, the single-user BER performance represents the upper-bound performance achievable, when multiple users are supported by the MIMO SCDMA system and, correspondingly, when multiuser detection is employed. Specifically, Fig. 3 shows the BER performance of the MIMO SCDMA system with respect to different number of multipath components, when assuming $V = 1$ or $V = 2$ receive antennas. The other parameters employed for Fig. 3 are shown on the top of the figure. From the results we observe that, for a given BER, the multipath diversity gain decreases, when increasing the number of receive antennas or the receiver diversity order. Specifically, at the BER of 10^{-4}, for the case

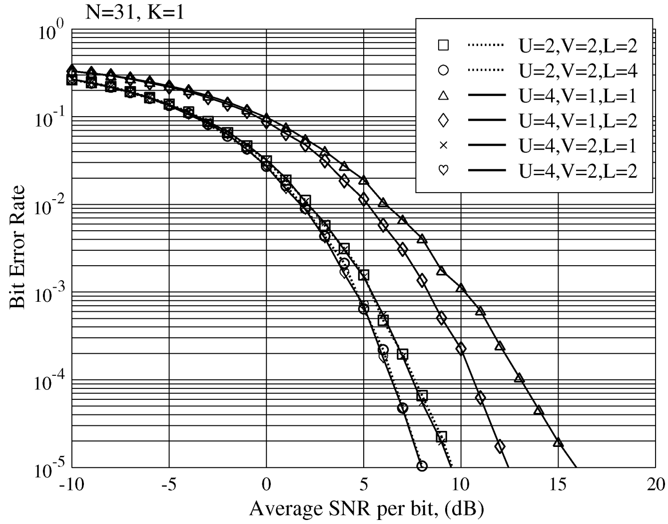

Fig. 4. BER performance of the single-user MIMO SCDMA system using $U = 2, 4$ transmit antennas, $V = 1$, two receive antennas, and $N = 31$ chips per bit duration, when communicating over Rayleigh-fading channels having $L = 1, 2$ multipath components.

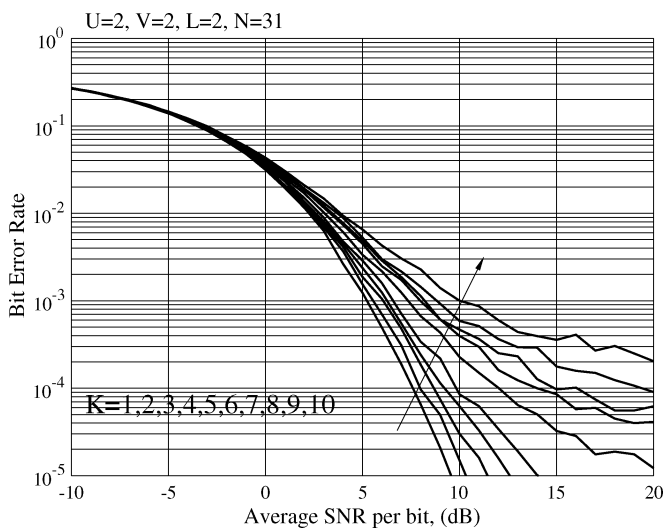

Fig. 5. BER performance of the multiuser MIMO SCDMA system when using **correlation detector** and when communicating over multipath Rayleigh-fading channels.

of using $V = 1$ receive antenna, the multipath diversity gain is about 8 dB, when the channel has $L = 5$ multipath components instead of $L = 1$. By contrast, when using $V = 2$ receive antennas, the multipath diversity gain reduces to about 3 dB for the same scenario.

In Fig. 4, the BER performance of the MIMO SCDMA system was evaluated and compared associated with various number of transmit antennas, multipath components, and receive antennas. From the results of Fig. 4, as well as the results in Figs. 3, we can be implied that the big-gap performance improvement can be achieved by deploying more receive antennas, especially, when the diversity order is already high. Furthermore, it can be shown from the results of Fig. 4 that both the transmit diversity and the multipath diversity have the same order of importance. As shown in Fig. 4, the BER performance of the cases corresponding to $U = 2$, $V = 2$,

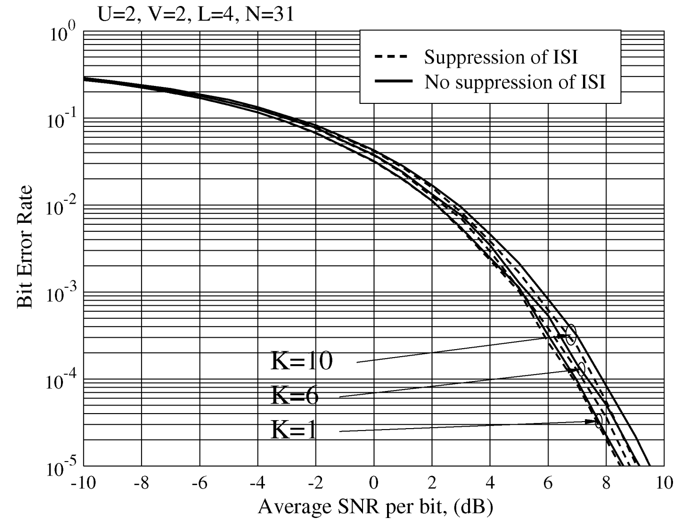

Fig. 6. BER performance of the multiuser MIMO SCDMA system when using **decorrelating detector** and when communicating over multipath Rayleigh-fading channels.

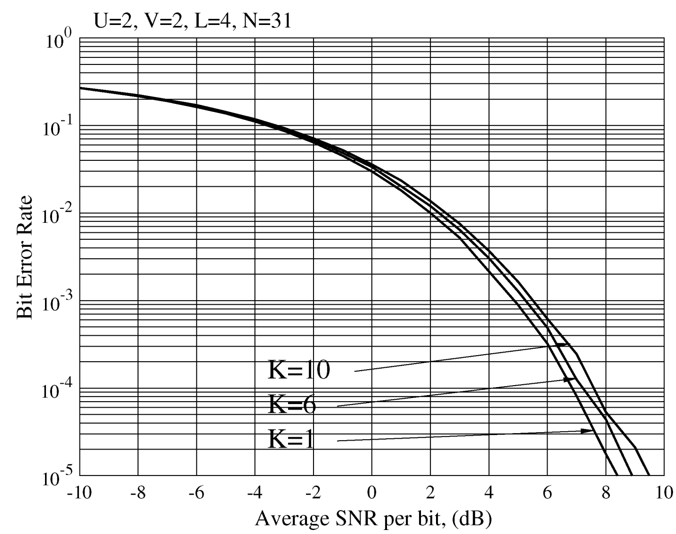

Fig. 7. BER performance of the multiuser MIMO SCDMA system when using **MMSE detector** and when communicating over multipath Rayleigh-fading channels.

$L = 2$, and $U = 2$, $V = 2$, $L = 4$ are the same as that of the cases corresponding to $U = 4$, $V = 2$, $L = 1$, and $U = 4$, $V = 2$, $L = 2$, respectively.

Fig. 5 shows the BER performance of the MIMO SCDMA system with respect to the number of users K, when the single-user correlation detector was considered. Since the correlation detector does not utilize the information from the other users including their code signatures and spatial signatures, explicitly, the BER performance becomes worse, when the MIMO SCDMA system supports more users. Furthermore, error-floors are observed in Fig. 5.

In Figs. 6 and 7, the BER performance of the MIMO SCDMA systems using multiuser detections were simulated, when the system supported $K = 1$, 6, and 10 users. Specifically, in Fig. 6, the decorrelating MUD was employed for detecting the multiuser signals, while in Fig. 7, the MMSE MUD was used. Note that, the decorrelating and MMSE algorithms are capable

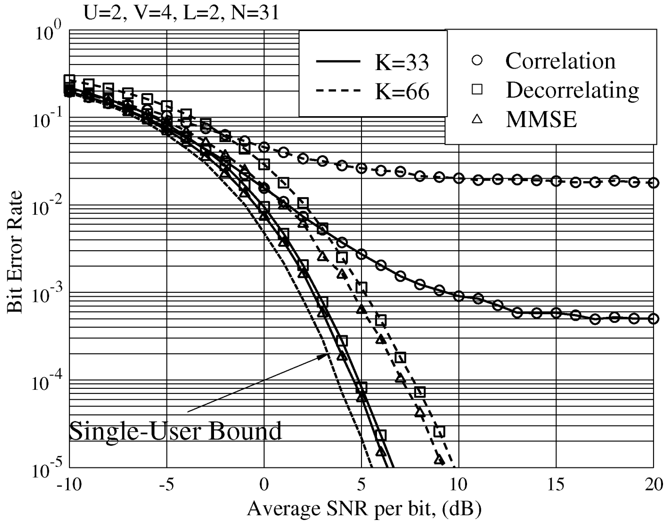

Fig. 8. BER performance comparison for the multiuser MIMO SCDMA system, when using **correlation**, **decorrelating**, and **MMSE** detectors and when communicating over multipath Rayleigh-fading channels.

of enhancing the BER performance, even when the MIMO SCDMA system supports only one user. This is because there exists multipath interference, when the MIMO SCDMA signal is transmitted over multipath fading channels. Furthermore, as noted in Section III, the decorrelating detection algorithm can be designed by either or not invoking the ISI signals. From the results of Figs. 6 and 7, we can find that, in comparison with the results of Fig. 5, both the decorrelating and MMSE detectors significantly outperform the correlation detector, and the error-floors existed in Fig. 5 can be efficiently removed by employing multiuser detection instead of single-user detection. Both the decorrelating and MMSE detectors are capable of achieving the near single-user performance bound, even the MIMO SCDMA system supports $K = 10$ users. Furthermore, from the results of Fig. 6, we observe that, when the ISI due to multipath transmission is invoked in the decorrelating detection, a better BER performance can be achieved, provided that the MIMO SCDMA signal has sufficient degrees of freedom for the ISI suppression.

Finally, in Fig. 8, we compared the BER performance of the three types of detectors, namely, correlation, decorrelating, and MMSE, considered in this contribution, when the MIMO SCDMA supported a relatively high number of users, which is $K = 33$ or 66. As we indicated at the beginning of this section, there are only 33 Gold sequences for a period of $N = 31$. Hence, when the MIMO SCDMA system supported $K = 66$ users, in our simulation each of the Gold sequences was assigned to two users. However, due to the independence of the spatial signatures of the two users sharing the same Gold sequence, as shown in Fig. 8, these two users can be successfully distinguished at a cost of about 3-dB SNR gain for both the decorrelating and the MMSE detectors. The reason for the loss of the 3-dB SNR gain is that the receiver has to use one receive antenna for suppressing the interfering signal sharing the same Gold sequence. Consequently, the receiver diversity order is reduced by one. The above observation implies that we can simply deploy more receiver antennas at the BS of an existing DS-CDMA system and treat the extended system as a SCDMA system, in order to increase the number of users supportable, while maintaining a similar BER performance of the existing DS-CDMA system. Additionally, from the results of Fig. 8, as in the literature [21], the MMSE MUD slightly outperforms the decorrelating detector.

V. Conclusion

In this contribution, we have proposed and investigated a MIMO SCDMA system, which combines both space-division and code-division, associated with using the STS transmit diversity scheme. Three low-complexity linear detectors have been considered. The BER performance of the MIMO SCDMA system associated with these linear detectors has been provided. From our study and simulation results, it can be shown that the MIMO SCDMA assisted by multiuser detection constitutes a highly promising multiple-access scheme, which is capable of efficiently exploiting the system resources and providing a high-flexibility. Furthermore, owing to its signaling structure, the proposed MIMO SCDMA constitutes one of the schemes that can be deployed in an existing DS-CDMA system with a relatively low-cost, in order to increase its capacity without demanding extra bandwidth. Our future work will endeavor to investigate low-complexity adaptive and blind adaptive MUDs for the MIMO SCDMA systems.

Acknowledgment

The author would like to acknowledge with thanks the financial assistance from EPSRC of UK, and professor Hsiao-Hwa Chen as well as the anonymous reviewers for their helpful comments.

References

[1] L. Hanzo, L.-L. Yang, E.-L. Kuan, and K. Yen, *Single- and Multi-Carrier DS-CDMA*. New York: Wiley, 2003.

[2] J. H. Winters, "On the capacity of radio communication systems with diversity in a Rayleigh fading environment," *IEEE J. Select. Areas Commun.*, vol. SAC-5, no. 5, pp. 871–878, Jun. 1987.

[3] I. E. Telatar, "Capacity of multiantenna Gaussian channels," *Eur. Trans. Telecommun.*, vol. 10, no. 6, pp. 585–595, Nov./Dec. 1999.

[4] D. Gesbert and M. Shafi *et al.*, "From theory to practice: An overview of MIMO space-time coded wireless systems," *IEEE J. Sel. Areas Commun.*, vol. 21, no. 3, pp. 281–302, Apr. 2003.

[5] A. Goldsmith, S. A. Jafar, N. Jindal, and S. Vishwanath, "Capacity limits of MIMO channels," *IEEE J. Sel. Areas Commun.*, vol. 21, no. 5, pp. 684–702, Jun. 2003.

[6] A. J. Paulraj, D. A. Gore, R. U. Nabar, and H. Bolcskei, "An overview of MIMO communications—A key to Gigabit wireless," *Proc. IEEE*, vol. 92, no. 2, pp. 198–218, Feb. 2004.

[7] "Special issue on MIMO systems and applications," *IEEE J. Sel. Areas Commun.*, vol. 21, no. 3, pp. 277–473, Apr. 2003.

[8] "Special issue on MIMO systems and applications," *IEEE J. Sel. Areas Commun.*, vol. 21, no. 4, pp. 481–673, May 2003.

[9] "Special issue on MIMO wireless communications," *IEEE Trans. Signal Process.*, vol. 51, no. 11, pp. 2709–2881, Nov. 2003.

[10] S. M. Alamouti, "A simple transmit diversity technique for wireless communications," *IEEE J. Sel. Areas Commun.*, vol. 16, no. 8, pp. 1451–1458, Oct. 1998.

[11] V. Tarokh, N. Seshadri, and A. R. Calderbank, "Space-time codes for high data rate wireless communication: Performance criterion and code construction," *IEEE Trans. Inf. Theory*, vol. 44, no. 2, pp. 744–765, Mar. 1998.

[12] J. H. Winters, "Optimum combining in digital mobile radio with cochannel interference," *IEEE J. Sel. Areas Commun.*, vol. SAC-2, no. 4, pp. 528–539, Jul. 1984.

[13] A. F. Naguib, A. Paulraj, and T. Kailath, "Capacity improvement with base-station antenna arrays in cellular CDMA," *IEEE Trans. Veh. Technol.*, vol. 43, no. 3, pp. 691–698, Aug. 1994.
[14] A. F. Naguib and R. Calderbank, "Space-time coding and signal processing for high data rate wireless communications," *Wireless Commun. Mobile Comput.*, vol. 1, no. 1, pp. 13–34, Jan.–Mar. 2001.
[15] J. M. F. Xavier, V. A. N. Barroso, and J. M. F. Moura, "Closed-form blind channel identification and source separation in SDMA systems through correlative coding," *IEEE J. Sel. Areas Commun*, vol. 16, no. 8, pp. 1506–1517, Oct. 1998.
[16] L.-L. Yang and L. Hanzo, "Performance of space-division multiple-access systems communicating over Nakagami-fading channels," in *Proc. IEEE Veh. Technol. Conf.-Spring*, Milan, Italy, May 2004, pp. 275–279.
[17] ——, "Minimum mean square error single-user detection of SDMA signals transmitted over Nakagami fading channels," in *Proc. IEEE Int Commun. Conf.*, Paris, France, Jun. 2004, pp. 2511–2515.
[18] B. Hochwald, T. L. Marzetta, and C. B. Papadias, "A transmitter diversity scheme for wideband CDMA systems based on space-time spreading," *IEEE J. Sel. Areas Commun.*, vol. 19, no. 1, pp. 48–60, Jan. 2001.
[19] L.-L. Yang and L. Hanzo, "Performance of broadband multicarrier DS-CDMA using space-time spreading-assisted transmit diversity," *IEEE Trans. Wireless Commun.*, vol. 4, no. 3, pp. 885–894, May 2005.
[20] R. Doostnejad, T. Lim, and E. Sousa, "Space-time spreading codes for a multiuser MIMO system," in *Proc. 36 Asilomar Conf. Signals, Syst., Comput.*, Nov. 2002, pp. 1374–1378.
[21] S. Verdu, *Multiuser Detection*. Cambridge, U.K.: Cambridge Univ. Press, 1998.
[22] R. E. Ziemer and R. L. Peterson, *Digital Communications and Spread Spectrum Systems*. New York: Macmillan, 1985.
[23] J. G. Proakis, *Digital Communications*, 3rd ed. New York: McGraw-Hill, 1995.
[24] H. L. V. Trees, *Optimum Array Processing*. New York: Wiley, 2002.
[25] Y.-P. Cheng, K.-Y. Zhang, and Z. Xu, *Matrix Theory*, 2nd ed. Xi'an, China: Northwesten Polytechnical Univ. Press, 2002.
[26] S. Haykin, *Adaptive Filter Theory*, 3rd ed. Upper Saddle River, NJ: Prentice-Hall, 1996.

Lie-Liang Yang (M'98–SM'02) received the B.Eng. degree in communication engineering from Shanghai TieDao University, Shanghai, China, in 1988, and the M.Eng. and Ph.D. degrees in communications and electronics from Northern Jiaotong University, Beijing, China, in 1991 and 1997, respectively.

From 1997 to 1997, he was a Visiting Scientist at the Institute of Radio Engineering and Electronics, Academy of Sciences of the Czech Republic. Since 1997, he has been with the Communications Research Group, School of Electronics and Computer Science, University of Southampton, Southampton, U.K., where he is a Member of the Academic Staff. He is currently an Editor for the *Journal of Communications and Networks* (JCN). He has published over 100 papers in journals and conference proceedings, coauthored one book, and published several book chapters. His research has covered a wide range of areas in telecommunications, which include error control coding, modulation and demodulation, spread-spectrum communications and multiuser detection, synchronization, smart antennas, adaptive wireless systems, as well as wideband, broadband, and ultra-wideband code-division multiple access (CDMA).

Dr. Yang was awarded the Royal Society Sino-British Fellowship in 1997 and the Engineering and Physical Sciences Research Council (EPSRC) Research Fellowship in 1998.